

Influence of Shielding Gas Composition on Structure and Mechanical Properties of Wire and Arc Additive Manufactured Inconel 625

IVAN JURIĆ,¹ IVICA GARAŠIĆ,¹ MATIJA BUŠIĆ ^{1,2} and ZORAN KOŽUH¹

1.—Faculty of Mechanical Engineering and Naval Architecture, University of Zagreb, Ivana Lučića 5, 10000 Zagreb, Croatia. 2.—e-mail: matija.busic@fsb.hr

Wire and arc additive manufacturing (WAAM) is becoming an increasingly important process for manufacture of components with complex geometry, being used for products made from expensive metals such as Inconel 625. The shielding gas used to protect the molten metal is one of the key process parameters due to its significant impact on the structure and mechanical properties of the final product. In this study, four samples were made using different shielding gas mixtures. Due to its high productivity, a metal active gas (MAG) welding process was used. Process stability and productivity rate were the main criteria used to determine the optimal range of welding parameters. Geometrical characteristics of the produced structures were analyzed. Finally, destructive tests were conducted on test specimens, and the data analyzed. The influence of the shielding gas composition on the structure and mechanical properties was determined, and conclusions are drawn.

INTRODUCTION

The share of small-series and single-unit production as well as customized manufacturing in overall production is constantly growing. The resulting large number of product variants poses many challenges to conventional production technologies. Reducing costs, shortening lead times, and improving product quality and flexibility in both development and manufacturing are therefore important areas for continuous improvement. Additive manufacturing (AM) is one of the modern technologies that can be an adequate response to these challenges, having great potential for reducing material waste, lead time, energy consumption, and lifecycle impacts.^{1,2} Compared with conventional machining processes for producing metallic structures, additive manufacturing can fabricate complex components at a high productivity level without expensive tools or the usual preproduction costs.^{3,4} Fabrication of components by depositing material layer-by-layer is the main characteristic of additive manufacturing, enabling production of complex geometries with close to net shape.⁵

Additive manufacturing processes can be classified according to the heat source applied, e.g., laser, electron beam, and arc, or the feedstock material used, e.g., powder and wire.⁶ Wire and arc additive manufacturing (WAAM) is an AM process that uses an electric arc to melt wire onto a substrate or previously deposited layer.² In comparison with powder-based AM processes, WAAM features a significantly higher material deposition rate and lower cost.^{7,8} The potentially limitless component size is another great advantage that makes the WAAM process superior to other AM processes.^{9–12} Since the WAAM process uses an electric arc to melt the wire, it is possible to apply a number of different welding processes. Due to the possibility of automation, commonly used welding processes include the tungsten inert gas (TIG), metal inert gas (MIG), and metal active gas (MAG) processes. MIG/MAG wire can provide additional material and act as the electrode at the same time, while its coaxiality with the welding gun makes it easier to determine the tool path.

Compared with conventional machining processes, WAAM provides considerable material savings because the final product can be made with less material waste. The ratio of the volume of the initial solid material (V_i) to the volume of the final product (V_f), is called the buy-to-fly (BTF) ratio, indicating how many times larger the volume of material used is relative to the volume of the product itself. The WAAM process can enable production of large products with complex geometry, achieving BTF ratios below 1.5.¹¹

As previously stated, WAAM is a promising technique for use in a number of industries due to its many advantages. However, several issues must be resolved to make WAAM suitable for such industrial applications.^{9–12} One of its drawbacks is the surface roughness, which affects the dimensions and quality of the produced part.^{11–13} The surface quality depends on several key parameters, including the arc stability, interlayer temperature, wire feed speed, travel speed, and constancy of the ratio of the wire feed speed to travel speed.¹⁴ The second limitation of the WAAM process is related to the residual stress in the produced part. Residual stresses generated during the process often lead to unacceptable distortion and significant degradation of mechanical properties.¹⁵ Residual stresses are generated by accumulation of cyclically repeated thermal expansion and contraction.¹⁶

Ni-based superalloys, such as Inconel 625, are used in diverse applications over a wide temperature range from cryogenic conditions to elevated temperature environments. Inconel 625 has high tensile strength, excellent corrosion and oxidation resistance, and fatigue strength in aggressive environments. Its ability to withstand high stress and a wide range of temperatures, both in and out of water, as well as to resist corrosion when exposed to highly acidic environments, makes it an appropriate choice for nuclear and marine applications. The strength of Inconel 625 derives from the stiffening effect of molybdenum and niobium in its nickel–chromium matrix, thus precipitation hardening treatment is not required. Although conventional manufacturing technologies can produce acceptable components, high production costs and complex geometries are recognized as factors limiting successful access of Inconel 625 components to the market. These are the reasons why many ongoing experiments are investigating use of WAAM to deposit this alloy.

The aim of the work presented herein is to determine the influence of different shielding gases on the microstructure and mechanical properties of Inconel 625 wall structures produced by WAAM with maximal productivity rate. Four types of shielding gas were utilized, all of which are normally used for welding of stainless steels or nickel alloys. The shielding gas used to protect the molten metal is one of the key process parameters, due to its significant impact on the microstructure and

mechanical properties of the final product. Process stability and productivity rate were the main criteria used to determine the optimal range of welding parameters. Geometrical characteristics of the produced structures were analyzed using three-dimensional (3D) scanning technology. Mechanical properties of the produced walls were compared with those of standard all-weld metal specified for the deposited material.

EXPERIMENTAL PROCEDURES

Component manufacturing was performed with an Almega OTC AX V6 welding robot and an OTC Daihen DP 400 welding machine using the MAG welding process. Welding parameters were selected considering the results of previous tests and information from literature. During WAAM of walls, welding parameters were measured along with the wall increase and interpass temperature. Layers were deposited on each other until a flat wall of certain height was obtained. X5CrNi18-10 stainless-steel plates with dimensions of 350 mm × 70 mm × 10 mm were used as base plates for material deposition. Inconel 625 wire (1.2 mm thick), designated as SNI6625 according to EN ISO 18274,¹⁷ was used as additive material. Table I presents the chemical composition of the selected wire according to the producer's specification. According to the same specification, the all-weld metal had tensile strength of 724 MPa and elongation of 30%. Four wall structures were produced using different welding parameters, i.e., heat input per layer and shielding gas:

- Wall 1 with Inoxline C2 (97.5% Ar and 2.5% CO₂)
- Wall 2 with Inoxline He3 H1 (95.5% Ar, 3% He, and 1.5% H₂)
- Wall 3 with Inoxline H5 (95% Ar and 5% H₂)
- Wall 4 with Argon 5.0 (99.999% Ar)

The short-circuiting metal transfer mode was used for WAAM of all samples. The welding speed for walls 1, 2, and 4 was 38 cm/min, while wall 3 was welded at speed of 36 cm/min due to the different stability of the process. The current was varied from 138 A to 130 A for wall 1, from 133 A to 119 A for wall 2, from 130 A to 121 A for wall 3, and from 131 A to 123 A for wall 4. The shielding gas

Table I. Chemical composition of SNI6625 wire

Element	wt.%	Element	wt.%
Ni + Co	58.0 min	Al	0.40 max
C	0.10 max	Ti	0.40 max
Mn	0.50 max	Cr	20.0–23.0
Fe	1.0 max	Nb + Ta	3.15–4.15
S	0.015 max	Mo	8.0–10.0
Cu	0.50 max	P	0.02 max
Si	0.50 max	Others	0.50 max

consumption was held constant at 19 l/min. The wire stick-out was 10 mm. The temperature was measured between layers using a Fluke 568 infrared (IR) thermometer. Each layer was deposited on the surface with temperature between 110°C and 120°C. Figure 1 shows the Inconel 625 wall structures produced by WAAM in this work.

The heat input was calculated according to the equation

$$Q = \frac{k \times U \times I \times 60}{v \times 1000} \text{ [kJ/cm]}$$

where U is the voltage, I is the current, v is the welding speed, and k is the coefficient of thermal efficiency of the specific welding process (0.8 for MAG). The average heat input of layers was as follows:

- 3.024 kJ/cm for wall 1
- 2.906 kJ/cm for wall 2
- 2.965 kJ/cm for wall 3
- 2.899 kJ/cm for wall 4.

Specimens for hardness testing, tensile strength testing, and geometric and macrostructure analysis were sectioned from the produced walls using a band saw. Specimens for tensile strength testing were sectioned in direction parallel to the direction of deposition and machined to the required dimensions according to the standard EN ISO 6892-1:2016.¹⁸ Tensile strength testing was conducted using a servohydraulic machine (VEB Werkstoffprufmaschinen GmbH, EU 40 mod). TIRAtest System software was used for processing of results.

Specimens for analysis of macrostructure and hardness measurement were ground using P120, P320, and P600 sandpapers. The ground specimens were then polished using a Pohenix Alpha Grinder polisher with water on P1000, P2000, and finally P4000 sandpapers. Polished specimens were electrochemically etched for 1 min at voltage of 8 V in a mixture of 10% oxalic acid ($C_2H_2O_4$) and 90% H_2O .

Geometric analysis was carried out on the side surface of the walls produced by WAAM. One specimen with dimensions of 60 mm × 60 mm was

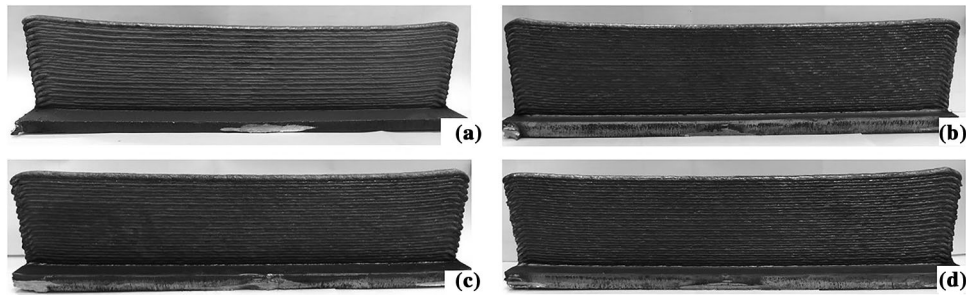


Fig. 1. (a) Wall 1, (b) wall 2, (c) wall 3, and (d) wall 4 produced by WAAM.

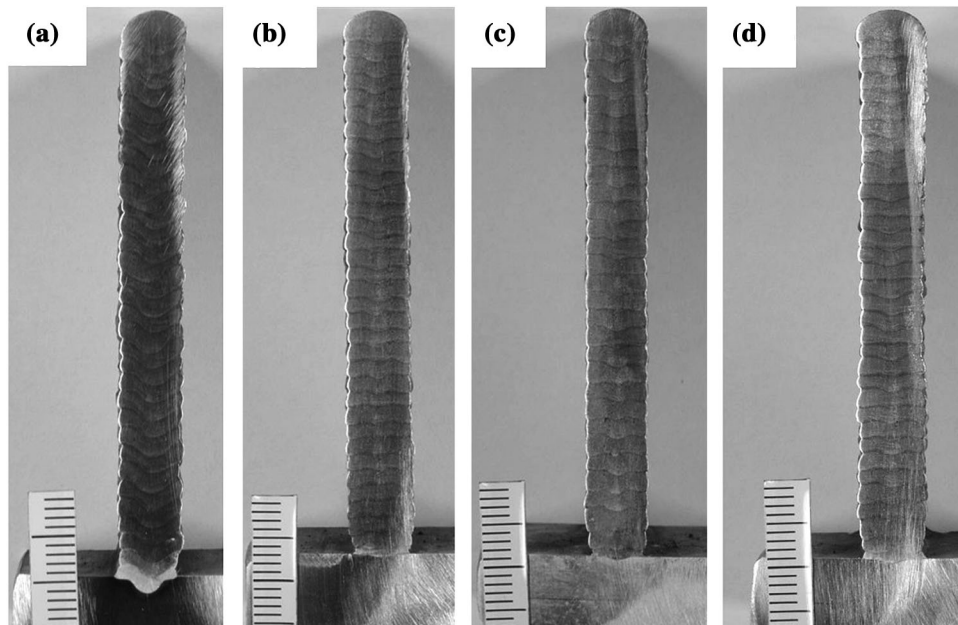


Fig. 2. Macrostructure of (a) wall 1, (b) wall 2, (c) wall 3, and (d) wall 4 produced by WAAM.

Table II. Results of tensile strength testing

Sample designation	$R_{p0.2}$ (MPa)	R_m (MPa)
TS 1	436.79	751.94
TS 2	354.32	698.13
TS 3	315.63	699.88
TS 4	336.25	698.99

sectioned from each produced wall. Only a surface area of 40 mm × 40 mm from each specimen was included in this analysis. Specimens were 3D scanned using a DAVID SLS-3 3D scanner with precision up to 0.1% of scan size (down to 0.06 mm). After scanning, stl files were obtained and processed using Mountainsmap Premium 7.4 software.

RESULTS AND DISCUSSION

Figure 2 shows the macrostructure of each produced wall. Using a robot as the torch guiding system resulted in excellent linearity and acceptable geometry of the walls. Optimal welding parameters and short-circuit metal transfer resulted in an effective wall width almost equal to the total wall width. Each layer could be clearly observed in macrosections of all the produced specimens. No imperfections or defects (lack of fusion, porosity, inclusions, etc.) were observed in the deposited layers. The waviness was smallest for sample 3 compared with the other samples.

Table II presents the results of tensile strength testing, clearly showing that only specimen TS 1 from wall 1 exhibited tensile strength above 724 MPa (the stated value for all-weld metal). The specimen sectioned from wall 1 reached 751.9 MPa, while the other specimens exhibited tensile strength of around 700 MPa. These measured values can only represent the tensile strength in the direction of material deposition.

Vickers HV10 hardness testing was performed on the surface of the wall cross-section according to Fig. 3. The positions of the measurements are scaled from the top of the wall down to the base plate. All measurement positions from 1 to 16 were located in the weld metal. The Vickers HV10 hardness test results are presented in Table III. The measured values varied from the top to the bottom of the sample due to the different locations of the measurement points in each layer (in the weld metal or near the heat-affected zone). The heat input during each pass will reheat previous passes throughout the whole wall, subjected them to a sort of heat treatment. From the measured results it is obvious that wall 1 showed the highest hardness in comparison with the other samples.

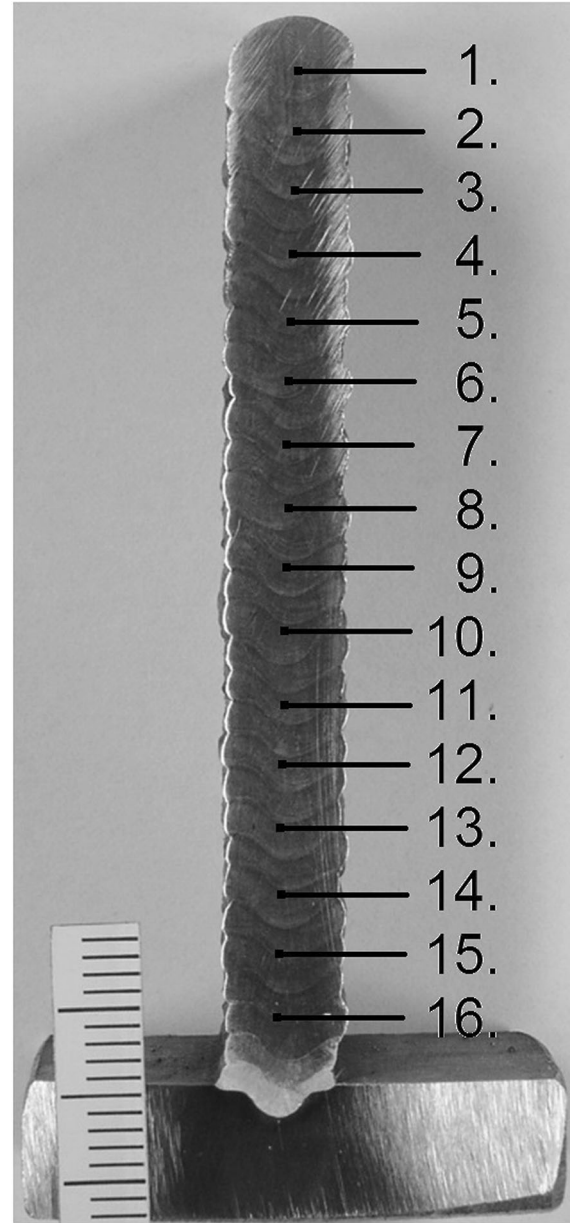


Fig. 3. Vickers HV10 hardness measurement positions.

Figure 4 presents the results of geometric analysis of the side surface on the walls produced by WAAM. The surface of samples 1 and 4 appeared rougher compared with samples 2 and 3, as confirmed by the statistical results. The root-mean-square height S_q and arithmetic mean height S_a were compared between all the samples. The wave heights were between 0.5 mm and 1 mm for samples 1 and 4. The wave heights of samples 2 and 3 were slightly smaller, between 0.35 mm and 0.7 mm.

Table III. Vickers HV10 hardness test results

Measurement position	Wall 1	Wall 2	Wall 3	Wall 4
1	232	203	193	191
2	228	213	193	198
3	230	210	206	192
4	218	205	206	201
5	228	206	212	198
6	233	203	199	205
7	221	218	194	197
8	221	206	202	199
9	222	203	192	201
10	216	210	206	194
11	225	215	196	205
12	225	206	210	206
13	228	209	207	206
14	222	224	199	206
15	209	233	210	205
16	212	245	213	202
Average	223.13	213.06	202.38	200.38

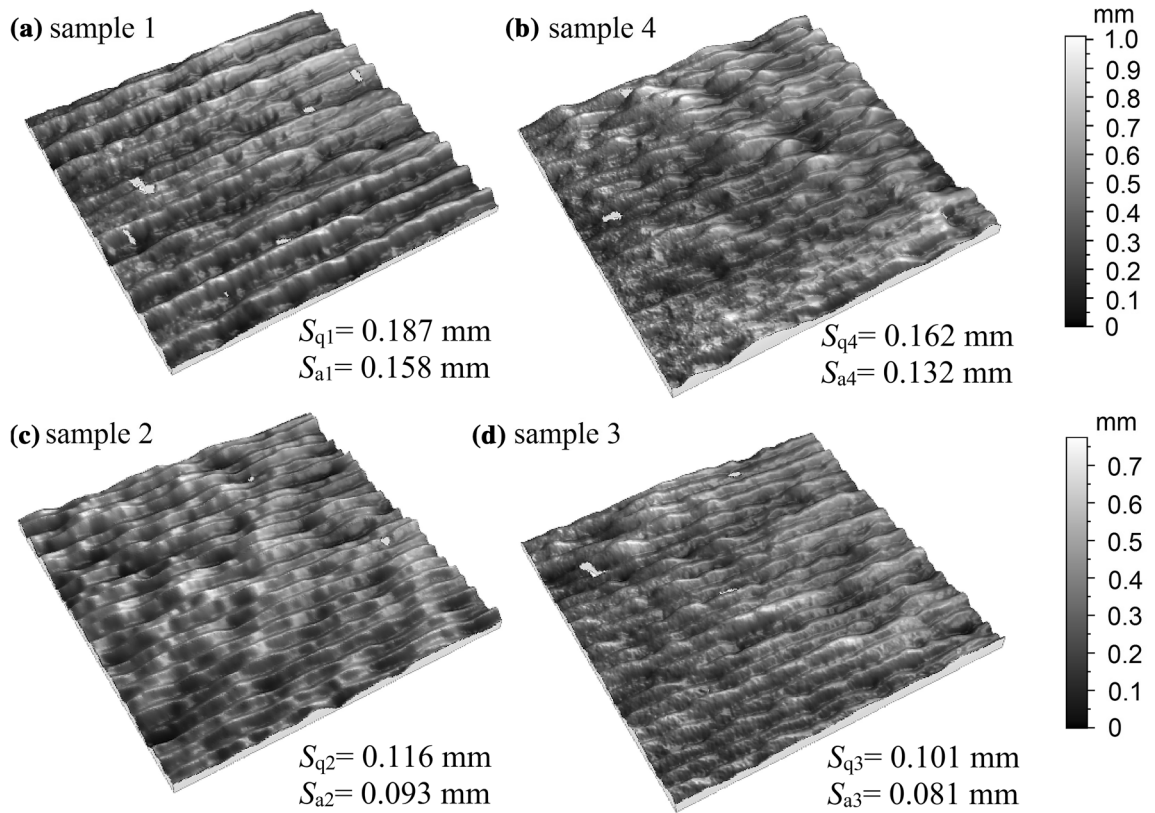


Fig. 4. Geometrical analysis of side surface on walls produced by WAAM: (a) sample 1 from wall 1, (b) sample 4 from wall 4, (c) sample 2 from wall 2, (d) sample 3 from wall 3.

CONCLUSION

The main aim of this work is to determine the influence of different shielding gases on the microstructure and mechanical properties of Inconel 625 wall structures produced by WAAM with a maximal productivity rate and maximal BTF ratio. From the obtained results, the following conclusions can be drawn:

- Macrostructure analysis confirmed an acceptable and homogeneous structure without visible defects. The used welding parameters (especially low heat input) and short-circuit metal transfer resulted in process stability, prevented molten metal leakage, and enabled uniform wall thickness along the height of the produced walls.
- 3D scanning of side surfaces of walls produced by WAAM showed that wall 1 had the poorest material deposition with significant waviness, which could be induced by the gas mixture containing oxygen from CO₂. The waviness of wall 3 was the smallest compared with the other samples. The waviness of all the samples was below 1 mm and should be acceptable for required future machining.
- Hardness measurements showed 10% higher values for wall 1 compared with the other samples. It can be concluded that WAAM of Inconel 625 alloy with shielding gas comprising 97.5% Ar and 2.5% CO₂ results in higher hardness in the cross-section of the produced wall. Additional heat treatment after WAAM of Inconel 625 can be recommended to equalize the hardness throughout the produced structure.
- Tensile strength testing showed that specimen TS 1 from wall 1 had tensile strength of 751.9 MPa, while other specimens exhibited values of around 700 MPa. It can be concluded that WAAM using 97.5% Ar and 2.5% CO₂ shielding gas resulted in the Inconel 625 wall with highest tensile strength compared with other shielding gases.
- It can be summarized that all of the studied gas mixtures could be applied during WAAM of Inconel 625 structures, but the shielding gas comprising 97.5% Ar and 2.5% CO₂ should result in production of structures with higher hardness

and tensile strength. However, the side surface of walls produced by WAAM using this shielding gas will probably have higher waviness and will require more machining to obtain a final product with flat surface.

ACKNOWLEDGEMENTS

This research was supported by COST Action CA15102 – “Solutions for Critical Raw Materials Under Extreme Conditions” (CRM-EXTREME).

REFERENCES

1. R. Huang, M. Riddle, D. Graziano, J. Warren, S. Das, S. Nimbalkar, J. Cresko, and E. Masanet, *J. Clean. Prod.* 135, 1559 (2016).
2. S.W. Williams, F. Martina, A.C. Addison, J. Ding, G. Pardal, and P. Colegrove, *Mater. Sci. Technol.* 32, 641 (2016).
3. A. Zinoviev, O. Zinovieva, V. Ploshikhin, V. Romanova, and R. Balokhonov, *Mater. Des.* 106, 321 (2016).
4. F. Liu, X. Lin, M. Song, H. Yang, K. Song, P. Guo, and W. Huang, *J. Alloys Compd.* 689, 225 (2016).
5. B.A. Szost, S. Terzi, F. Martina, D. Boisselier, A. Prytuliak, T. Pirling, M. Hofmann, and D.J. Jarvis, *Mater. Des.* 89, 559 (2015).
6. Y. Oguzhan and A.U. Adnan, *Proc. Inst. Mech. Eng. B J. Eng. Manuf.* 230, 1781 (2016).
7. B. Yin, H. Ma, J. Wang, K. Fang, H. Zhao, and Y. Liu, *Mater. Lett.* 190, 64 (2016).
8. D. Ding, Z. Pan, S.V. Duin, H. Li, and C. Shen, *Materials* 9, 652 (2016).
9. F. Martina, M.J. Roy, B.A. Szost, S. Terzi, P.A. Colegrove, S.W. Williams, P.J. Withers, J. Meyer, and M. Hofmann, *Mater. Sci. Technol.* 32, 1439 (2016).
10. F. Martina and S. Williams, Report: Welding Engineering and Laser Processing Centre, ver. 1.0, 2015, Cranfield University (2015).
11. A. Busachi, A.J. Erkoyuncu, F. Martina, and J. Ding, *Proc. CIRP* 37, 48 (2015).
12. R. Sun, L. Li, Y. Zhu, W. Guo, P. Peng, B. Cong, J. Sun, Z. Che, B. Li, C. Guo, and L. Liu, *J. Alloys Compd.* 747, 255 (2018).
13. Y. Li, Q. Han, G. Zhang, and I. Horváth, *Int. J. Adv. Manuf. Technol.* 96, 3331 (2018).
14. J. Xiong, Y. Li, R. Li, and Z. Yin, *J. Mater. Process. Technol.* 252, 128 (2018).
15. J. Ding, P.A. Colegrove, J. Mehnen, S. Ganguly, P.M. Sequeira Almeida, F. Wang, and S. Williams, *Comput. Mater. Sci.* 50, 3315 (2011).
16. R.J. Moat, A.J. Pinkerton, L. Li, P.J. Withers, and M. Preuss, *Mater. Sci. Eng. A* 528, 2288 (2011).
17. EN ISO 18274:2010 Welding consumables—solid wire electrodes, solid strip electrodes, solid wires and solid rods for fusion welding of nickel and nickel alloys—classification.
18. EN ISO 6892-1:2016 Metallic materials—tensile testing—part 1: method of test at room temperature.